

KAZAN (VOLGA REGION) FEDERAL UNIVERSITY

INSTITUTE OF PHYSICS

Department of radioelektronic

KUSHTANOVA G. G.

WELL TEST ANALYSIS

Teaching textbook for the course of lectures

Kazan 2015

УДК 532.546

*Принято на заседании кафедры радиоэлектроники
Протокол № 4 от 23 января 2015 года
Утверждено на методической комиссии института физики
протокол № 11 от 12 марта 2015 года*

Рецензент

Зав. лаб. подземной гидродинамики ИММ КазНЦ РАН, д.т.н., профессор,
действительный член РАЕН Хайруллин М.Х.

Title: Well test analysis: teaching textbook for the course of lectures / G.G. Kushtanova – Kazan: Kazan University, 2014. – P. 31.

The teaching textbook for the course of lectures discusses the well tests analysis. The new interpretation methods, using the derivative of the pressure, magnify the characteristic features of the many different types of wells and reservoirs. Focus is placed on computerized interpretation of complex systems. The interpretation software packages have been used for the preparation of the color Figures: SAPHIR of KAPPA Engineering

This study guide will be useful for students, graduate students, postgraduate students as well as for the researchers in the field of the well test analysis and hydrodynamic studies of reservoir.

© Kushtanova G. G., 2015

© Kazan University, 2015

Contents

TYPICAL FLOW REGIMES AND SAME CONCEPTS	4
Skin	4
Radius of investigation.....	5
Drawdown and build-up test	6
Wellbore storage effect	6
Flow pattern	8
<i>Radial</i>	8
<i>Spherical, half-spheric (hemispherical)</i>	10
<i>Fractured well (infinite conductivity fracture): linear flow regime</i>	11
<i>Fractured well (finite conductivity fracture): bi-linear flow regime</i>	12
<i>Well in partial penetration: spherical flow regime</i>	13
Bourdet derivative	15
Well with wellbore storage and skin in a homogeneous reservoir.....	16
EFFECT OF RESERVOIR BOUNDARIES	17
Single sealing fault un homogeneous reservoir.....	17
Two parallel sealing faults	18
Two intersecting sealing fault	18
Constant pressure boundary	19
Closed reservoir	19
EFFECT OF RESERVOIR HETEROGENEITIES	20
Double porosity (porous-fractured reservoir).....	20
Composite reservoir	21
Infinite conductivity or uniform flux vertical fracture	22
WELLBORE CONDITIONS.....	23
Finite conductivity vertical fracture	23
Horizontal well.....	24
Changed wellbore storage	27
STEP RATE TEST FOR PRODUCING WELL	28
NOMENCLATURE.....	29
BIBLIOGRAPHY	30
SUMMARY	30
APPENDIX	31

WELL TEST ANALYSIS: THE USE OF BOURDET'S DERIVATIVE

This material taken from the book (Bourdet, 2002). The interpretation software packages have been used for the preparation of the color Figures: SAPHIR of KAPPA Engineering, provided by free academic license.

The relations with the numbers "a" are in oilfield units, with the numbers "b" - in metric units.

TYPICAL FLOW REGIMES AND SOME CONCEPTS

Steady state

During steady-state flow, the pressure does *not change* with time.

$$\frac{\partial p}{\partial t} = 0$$

Pseudo steady state

The pseudo steady state regime characterizes a closed system response. With a constant rate production, the drop of pressure becomes *constant* for each unit of time.

$$\frac{\partial p}{\partial t} = \text{constant}$$

using the method of indicator diagram can analyze load and displacement of suspension point, calculate liquid producing capacity at the mouth of a well, achieve a real-time, continuous and automatic measurement of liquid producing capacity.

Transient state

Transient responses are observed before constant pressure or closed boundary effects are reached. The pressure variation with time is a function of the well geometry and the reservoir properties, such as permeability and heterogeneity.

$$\frac{\partial p}{\partial t} = f(x, y, z, t)$$

Usually, well test interpretation focuses on the transient pressure response. Near wellbore conditions are seen first and later, when the drainage area expands, the pressure response is characteristic of the reservoir properties until boundary effects are seen at late time (then the flow regime changes to pseudo steady or steady state).

Skin

In the case of a damaged well, a flow restriction is present at the interface between the reservoir and the wellbore, producing an *additional* pressure drop Δ

P_{skin} when the fluid enters into the well. For a stimulated well, the flowing condition is improved near the well, and the pressure decline is *reduced* in a cylindrical near wellbore reservoir region.

The same skin can describe a low or very high damage, depending on the flow rate and the reservoir permeability. The skin factor S is a *dimensionless parameter* (van Everdingen 1953), and it characterizes the well condition: for a damaged well $S > 0$ and, by extension, $S < 0$ for a stimulated well.

Typical examples of a *damaged well* ($S > 0$) are poor contact between the well and the reservoir (mud-cake, insufficient perforation density, partial penetration) or invaded zone.

Stimulated well ($S < 0$) behavior is observed when the surface of contact between the well and the reservoir has been increased compared to the basic cylindrical vertical wellbore geometry (fractured well, slanted and horizontal well) or acid stimulated zone.

$$S = \left(\frac{k}{k_s} - 1 \right) \ln \frac{r_s}{r_w}$$

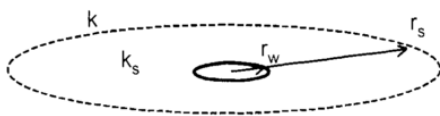


Figure 1. Flow through a circular reservoir region.

The equivalent wellbore radius is defined with

$$r_{we} = r_w e^{-S}$$

A common well stimulation method consists of creating a hydraulic vertical fracture from the wellbore to the formation. The reservoir / well surface of contact is significantly increased, thus producing a negative skin factor.

Fracturing greatly exaggerate productivity index of well. The flow can be considered as pseudoradial with negative skin.

Effective radius for fracture is equal to half of the half fracture length.

- Insufficient perforation density $S > 0$
Perforation holes penetrates in intact zone (microfractures) $S < 0$.
- Horizontal well – as vertical well with negative skin, in consequence of surface contact area increasing.
- Gas well – non Darcy flow. Additional pressure drop produced by turbulent flow. $S > 0$.
- Skin in injection well: injection involve changing of coefficient of mobility (k/μ) in well bottom zone aaaaand additional pressure drop.
- Geologocal skin – well drill low- or high-permeable reservoir.

Radius of investigation

$$r_i = 0.032 \sqrt{\frac{k\Delta t}{\phi\mu c_t}} \quad (1a)$$

$$r_i = 0.037 \sqrt{\frac{k\Delta t}{\phi\mu c_t}} \quad (1b)$$

Drawdown and build-up test

Before opening, the initial pressure p_i is constant and uniform in the reservoir. During the flowing period, the drawdown pressure response Δp is defined as follows:

$$\Delta p = p_i - p(t)$$

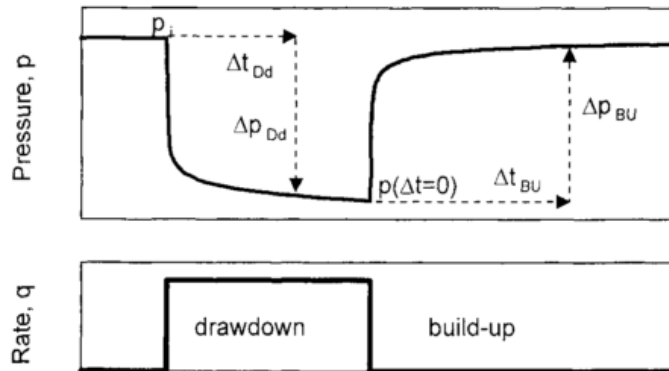


Figure 2. Drawdown and build-up test sequence.

When the well is shut-in, the build-up pressure change Δp is estimated from the last flowing pressure $p(\Delta t=0)$:

$$\Delta p = p(t) - p(\Delta t = 0)$$

The pressure response is analyzed versus the elapsed time Δt since the start of the period (time of opening or shut-in).

Wellbore storage effect

The well is assumed to be vertical and to penetrate the complete reservoir thickness. Wellbore storage effect and possibly an infinitesimal skin are present.

Wellbore storage, also called afterflow, afterproduction.

When a well is opened, the production at surface is initially due to the *expansion* of the fluid stored in the wellbore, and the reservoir contribution is initially negligible. This characteristic flow regime, called the *pure wellbore storage effect*, can last from a few seconds to a few minutes. Then, the reservoir production starts and the sand face rate increases until it becomes the same as the surface rate. When this condition is reached, the wellbore storage has no effect any more on the bottom hole pressure response, the data describes the reservoir behavior and it can be used for transient analysis.

During shut-in periods, the wellbore storage effect is also called *afterflow*: after the well has been shut-in, the reservoir *continues to produce* at the sand face and the fluid stored in the wellbore is recompressed. The same sequence with three different pressure behaviors can be observed: the pure wellbore storage effect, transition when the sand face rate declines, and the end of the wellbore storage effect when the sand face rate becomes negligible and eventually zero.

After any change in the well flowing conditions, there is a time lag between the surface production and the sand face rate. The effect of wellbore storage affects well pressure responses during the first instants of each test period.

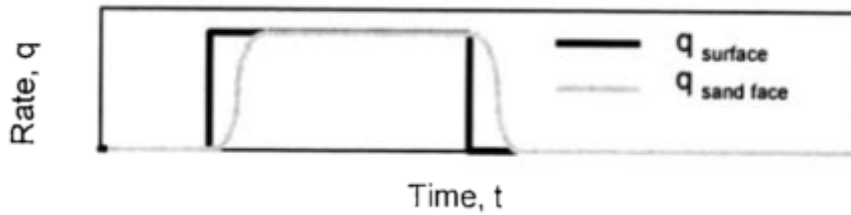


Figure 3. Wellbore storage effect. Sand face and surface rates.

Wellbore storage coefficient

The wellbore storage coefficient defines the rate of pressure change during the pure wellbore storage regime.

where:

C_o : liquid compressibility

V_w : wellbore volume in Bbl

During the pure wellbore regime, the well is acting as a closed volume and, with a constant surface rate condition, the pressure changes linearly with time. The wellbore storage coefficient can be estimated on a plot of the pressure change Δp versus the elapsed time Δt time on a *linear scale*.

At early time, the response follows a straight line of slope m_{wBS} , intercepting the origin.

$$\Delta p = \frac{qB}{24C} \Delta t$$

The *wellbore storage coefficient* C is estimated from the straight-line slope m_{wBS} : $C = \frac{qB}{24m_{wBS}}$

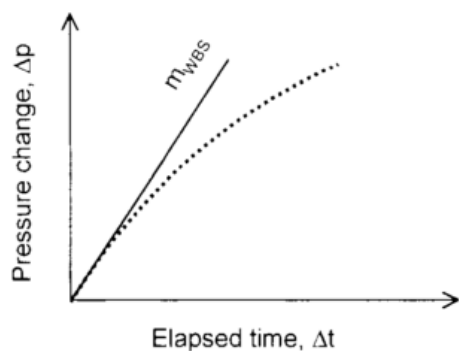


Figure 4. Wellbore storage effect. Specialized analysis on a linear scale.

Flow pattern

Radial

When the reservoir production is established, the flow-lines converge towards the well with a radial geometry. In the reservoir, the pressure is a function of the *time* and the *distance* to the well. As the production time increases, the well bottom-hole pressure p_{wf} drops, and the circular drainage area of radius r_i expands in the reservoir.

During the radial flow regime in reservoirs with homogeneous behavior, the pressure changes with the logarithm of the elapsed time from when the well is opened (Miller et al., 1950). A plot of the bottom hole pressure versus the logarithm of time (called MDH plot) follows a straight line when all wellbore storage transitional effect are finished. The slope m of semi-log straight line is used to estimate the reservoir permeability thickness product kh , and the skin coefficient S is evaluated from the location of the straight line along the y-axis.

$$\Delta p = 162.6 \frac{qB\mu}{kh} \left[\log \Delta t + \log \frac{k}{\phi \mu c_t r_w^2} - 3.23 + 0.87S \right] \quad (2a)$$

$$\Delta p = 21.5 \frac{qB\mu}{kh} \left[\log \Delta t + \log \frac{k}{\phi \mu c_t r_w^2} - 3.10 + 0.87S \right] \quad (2b)$$

Traditionally, the semi-log straight-line location is characterized by the straight-line pressure at 1 hour

$$k = 162.6 \frac{qB\mu}{m} \quad (3a)$$

$$k = 21.5 \frac{qB\mu}{m} \quad (3b)$$

$$S = 1.151 \left[\frac{\Delta p_{1hr}}{m} - \log \frac{k}{\phi \mu c_t r_w^2} + 3.23 \right] \quad (4a)$$

$$S = 1.151 \left[\frac{\Delta p_{1hr}}{m} - \log \frac{k}{\phi \mu c_t r_w^2} + 3.10 \right] \quad (4b)$$

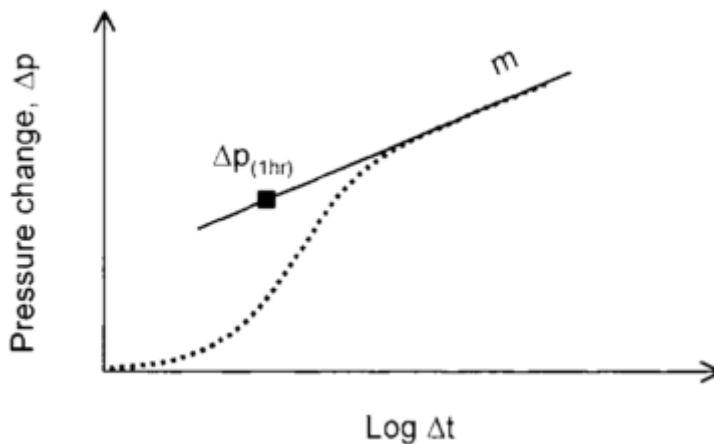


Figure 5. Radial flow regime. Specialized analysis on semi-log scale.

Shut-in periods

Drawdown periods are in general not suitable for analysis because it is difficult to ascertain a constant flow rate. The response is distorted, especially with the log-log scales that expand the response at early time. Preferably, build-up periods are used where the flow rate is zero, therefore the well is controlled.

Build-up responses do not show the same behavior as the first drawdown in a virgin reservoir at initial pressure. After a flow period of duration t_p , the well shows a pressure drop of $\Delta p(t_p)$. In the case of an infinite reservoir, after shut-in it takes an infinite time to reach the initial pressure during build-up, and to produce a pressure change $\Delta p_{BU}(t=\infty)$ of magnitude $\Delta p(t_p)$. As described on Figure 2.4, the shape of pressure build-up curves depends upon the previous rate history.

The diffusivity equation used to generate the well test analysis solutions is linear. It is possible to add several pressure responses, and therefore to describe the well behavior after any rate change. This is the superposition principle (van Everdingen and Hurst, 1949). For a build-up after a single drawdown period at rate q during t_p , the rate history is changed by superposing an injection period at rate $-q$ from time t_p , to the flow period from time $t=0$ extended into the shut-in times $t_p + \Delta t$

Using the superposition principle, build-up type curves can be generated for any production history. In the case of Figure 2.5 with a single constant rate drawdown of t_p before shut-in, the build-up type curve $p_{BUD}(\Delta t)_D$ is simply obtained by subtracting the quantity

$$p_D(t_p + \Delta t)_D - p_D(\Delta t)_D$$

from the pressure change at the time of shut-in $p_D(t_p)_D$

$$\Delta p_{BU}(\Delta t)_D = p_D(\Delta t)_D - p_D(t_p + \Delta t)_D + p_D(t_p)_D$$

$$\Delta p_{BU}(\Delta t) = 162.6 \frac{qB\mu}{kh} \left[\log \frac{t_p \Delta t}{t_p + \Delta t} + \log \frac{k}{\phi \mu c_t r_w^2} - 3.23 + 0.87S \right] \quad (5a)$$

$$\Delta p_{BU}(\Delta t) = 21.5 \frac{qB\mu}{kh} \left[\log \frac{t_p \Delta t}{t_p + \Delta t} + \log \frac{k}{\phi \mu c_t r_w^2} - 3.10 + 0.87S \right] \quad (5b)$$

With the superposition time, the build-up correction method compresses the time scale.

Horner method

With the Homer method (1951), a simplified superposition time is used: the constant t_I is ignored, and the shut-in pressure is plotted as a function of $\log((t_p + \Delta t)/\Delta t)$. On the Homer scale, the shape of the build-up response is symmetrical to that of the superposition plot Figure 2.7, early time data is on the right side of the plot (large Homer time) and, at infinite shut-in time, $(t_p + \Delta t)/\Delta t$

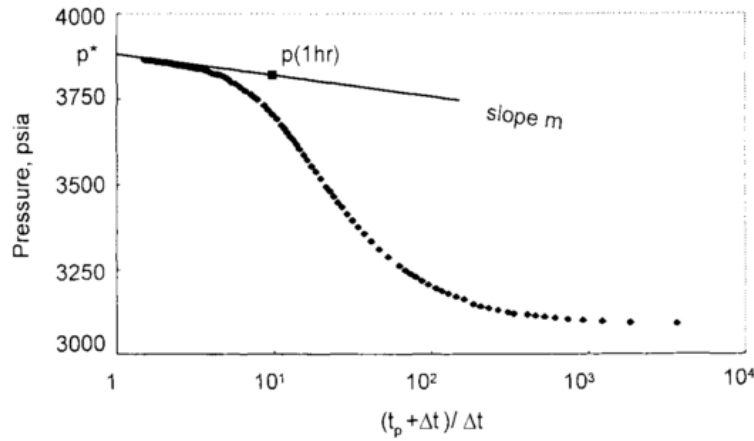


Figure 6. Horner plot of build-up example.

$$p_{ws} = p_i - 162.6 \frac{qB\mu}{kh} \log \frac{t_p + \Delta t}{\Delta t} \quad (6a)$$

$$p_{ws} = p_i - 21.5 \frac{qB\mu}{kh} \log \frac{t_p + \Delta t}{\Delta t} \quad (6b)$$

On a Horner plot of build-up data, the straight line slope m , the pressure at 1 hour on the straight line $\Delta p(\Delta t = 1 \text{ hr})$, and the extrapolated straight line pressure p^* at infinite shut-in time ($\Delta t = \infty$) are estimated. The results of analysis are:

$$k = 162.6 \frac{qB\mu}{m} \quad (3a)$$

$$k = 21.5 \frac{qB\mu}{m} \quad (3b)$$

$$S = 1.151 \left[\frac{\Delta p_{1hr}}{m} - \log \frac{k}{\phi \mu c_t r_w^2} + \log \frac{t_p + 1}{t_p} + 3.23 \right] \quad (7a)$$

$$S = 1.151 \left[\frac{\Delta p_{1hr}}{m} - \log \frac{k}{\phi \mu c_t r_w^2} + \log \frac{t_p + 1}{t_p} + 3.10 \right] \quad (7b)$$

In an infinite system, the straight line extrapolates to the initial pressure and $p^* = p_i$. When the production time is large compared to the shut-in time $t_p \gg \Delta t$, the Horner time can be simplified with:

$$\log \frac{t_p + \Delta t}{\Delta t} \approx \log t_p - \log \Delta t$$

The compression of the time scale becomes negligible, the Horner straight-line slope m is independent of the production time and the build-up data can be analyzed on a MDH semi-log scale.

Spherical, half-spheric (hemispherical)

With a well in partial penetration, the well is connected to the producing interval on one fraction only of the zone thickness. The reservoir / well surface of contact being reduced, partially

penetrating wells are characterized by a positive skin factor. In the following, this well configuration is introduced to illustrate another example of characteristic flow regime.

The ratio h_w/h of the length of the perforated interval to the formation thickness is called the penetration ratio, k_H and k_V -are the horizontal and vertical permeability.

In a well in partial penetration, after an initial radial flow regime in front of the perforated interval, the flow lines are established in both the horizontal and vertical directions, until the top and bottom boundaries are reached. A *spherical flow* regime can thus be observed before the flow becomes radial in the complete formation thickness.

Fractured well (infinite conductivity fracture): linear flow regime

A common well stimulation method consists of creating a hydraulic vertical fracture from the wellbore to the formation. The reservoir / well surface of contact is significantly increased, thus producing a negative skin factor. Two main types of fractured well behavior are observed: infinite or finite conductivity fracture.

The fracture is symmetrical on both sides of the well and it intercepts the complete formation thickness, x_f is the half fracture length. With the infinite conductivity fracture model, it is assumed that the fluid flows along the fracture without any pressure drop.

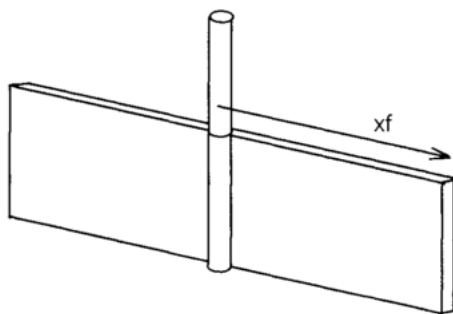


Figure 7. Fractured well. Fracture geometry.

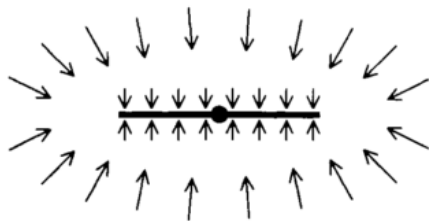


Figure 8. Infinite conductivity fracture. Geometry of the flow lines. Linear and pseudo radial flow regimes.

At early time, the flow-lines are perpendicular to the fracture plane. This is called a linear flow regime. Later, the reservoir regions at the two ends of the fracture starts to contribute significantly to the flow, the linear flow regime ends, to change into an elliptical flow geometry. Ultimately, the well response shows the characteristic radial flow regime behavior. During linear

flow, the pressure change is proportional to the square root of the elapsed time since the well was opened (Clark, 1968 and Gringarten et al., 1974 a).

$$\Delta p = 4.06 \frac{qB}{hx_f} \sqrt{\frac{\mu}{\phi k c_t}} \sqrt{\Delta t} \quad (8a)$$

$$\Delta p = 0.623 \frac{qB}{hx_f} \sqrt{\frac{\mu}{\phi k c_t}} \sqrt{\Delta t} \quad (8b)$$

The linear flow regime can be analyzed with a plot of the pressure change Δp versus the square root of elapsed time $\sqrt{\Delta t}$ the response follows a straight line of slope m_{LF} , intercepting the origin. When the reservoir permeability is known from the analysis of the subsequent radial flow regime, the slope m_{LF} of the linear flow straight line is used to estimate the half fracture length x_f .

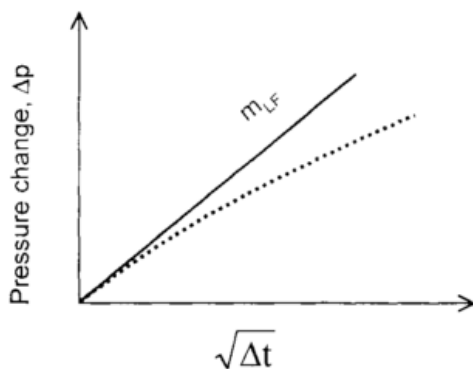


Figure 9. Infinite conductivity fracture.

Specialized analysis with the pressure versus the square root of time

$$x_f = 4.06 \frac{qB}{hm_{LF}} \sqrt{\frac{\mu}{\phi k c_t}} \quad (9a)$$

$$x_f = 0.623 \frac{qB}{hm_{LF}} \sqrt{\frac{\mu}{\phi k c_t}} \quad (9b)$$

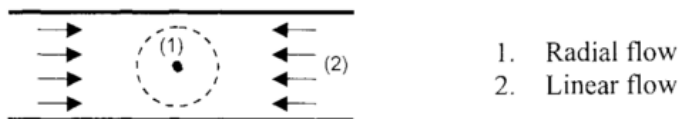


Figure 10. Example of a well in a channel reservoir.

Fractured well (finite conductivity fracture): bi-linear flow regime

When the pressure drop in the fracture plane is not negligible, a second linear flow regime is established along the fracture extension. Before the two ends of the fracture are reached, this well configuration produces the so-called bi-linearflow regime.

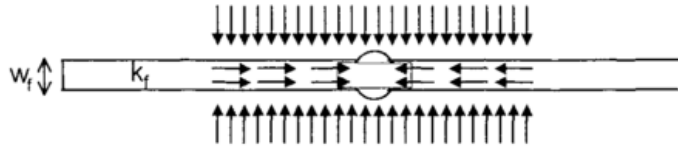


Figure 11. Finite conductivity fracture. Geometry of the flow lines during the bi-linear flow regime.

During bilinear flow, the pressure change is proportional to the fourth root of the elapsed time since the well was opened (Cinco-Ley et al., 1978). With w_f the width of the finite conductivity fracture and k_f the permeability in the fracture:

$$\Delta p = 44.11 \frac{qB\mu}{h\sqrt{k_f}w_f^4\sqrt{\phi\mu c_t k}} \sqrt[4]{\Delta t} \quad (10a)$$

$$\Delta p = 6.28 \frac{qB\mu}{h\sqrt{k_f}w_f^4\sqrt{\phi\mu c_t k}} \sqrt[4]{\Delta t} \quad (10b)$$

On a plot of the pressure change Δp versus the fourth root of elapsed time $\sqrt[4]{t}$, pressure response follows a straight line of slope m_{BLF} , intercepting the origin, during the bilinear flow regime

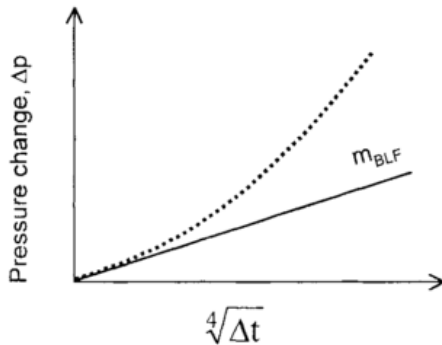


Figure 12. Finite conductivity fracture. Specialized analysis with the pressure versus the fourth root of time.

As for the linear flow analysis, provided the reservoir permeability can be estimated from semi-log analysis of the late time response, the slope m_{BLF} of the bilinear flow straight line is used to estimate the controlling parameter, namely the fracture conductivity $k_f w_f$:

$$k_f w_f = 1944.8 \sqrt{\frac{1}{\phi\mu c_t k}} \left(\frac{qB\mu}{hm_{BLF}} \right)^2 \quad (11a)$$

$$k_f w_f = 39.46 \sqrt{\frac{1}{\phi\mu c_t k}} \left(\frac{qB\mu}{hm_{BLF}} \right)^2 \quad (11b)$$

Well in partial penetration: spherical flow regime

With a well in partial penetration, the well is connected to the producing interval on one fraction only of the zone thickness. The reservoir / well surface of contact being reduced, partially penetrating wells are characterized by a positive skin factor. In the following, this well

configuration is introduced to illustrate another example of characteristic flow regime. The ratio h_H/h of the length of the perforated interval to the formation thickness is called the penetration ratio, k_H and k_V are the horizontal and vertical permeability (Figure 1.16).

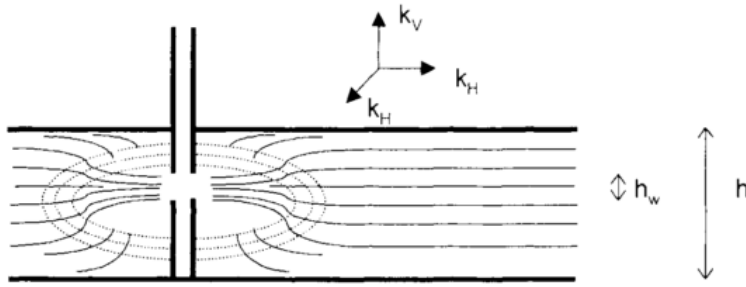


Figure 13. Well in partial penetration. Geometry of the flow lines. Radial, spherical and radial flow regimes.

In a well in partial penetration, after an initial radial flow regime in front of the perforated interval, the flow lines are established in both the horizontal and vertical directions, until the top and bottom boundaries are reached. A spherical flow regime can thus be observed before the flow becomes radial in the complete formation thickness.

During the spherical flow regime, the pressure changes with $1/\sqrt{\Delta t}$.

$$\Delta p = 70.6 \frac{qB\mu}{k_{SR}S} - 2452.9 \frac{qB\mu\sqrt{\phi\mu c_t k}}{k_S^{3/2}\sqrt{\Delta t}} \quad (12a)$$

$$\Delta p = 9.33 \frac{qB\mu}{k_{SR}S} - 279.3 \frac{qB\mu\sqrt{\phi\mu c_t k}}{k_S^{3/2}\sqrt{\Delta t}} \quad (12b)$$

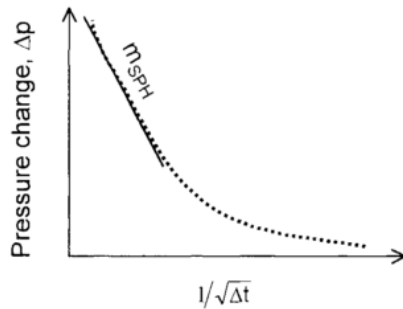


Figure 14. Well in partial penetration. Specialized analysis with the pressure versus 1/the square root of time.

Where k_S is the spherical permeability defined as

$$k_S = \sqrt[3]{k_x k_y k_z} = \sqrt[3]{k_H^2 k_V}$$

Specialized analysis

On a plot of the pressure versus the reciprocal of the square root of time, a straight line of slope m_{SPH} develops during the spherical flow regime. The spherical permeability k_S can be estimated with:

$$k_S = \left(2452.9 \frac{q_B \mu \sqrt{\phi \mu c_t k}}{m_{SPH}} \right)^{2/3} \quad (13a)$$

$$k_S = \left(279.3 \frac{q_B \mu \sqrt{\phi \mu c_t k}}{m_{SPH}} \right)^{2/3} \quad (13b)$$

Bourdet derivative

Log-Log scale

The dimensionless pressure p_D and time t_D are linear functions of Δp and Δt , the coefficients A and B being dependent upon different parameters such as the permeability k .

$$p_D = A \Delta p, \quad A = f(kh, \dots)$$

$$t_D = B \Delta t, \quad B = g(k, C, S, \dots)$$

On log-log scales, the shape of the response curve is characteristic: the product of one of the variables by a constant term is changed into a displacement on the logarithmic axes. If the flow rate is doubled, for example, the amplitude of the response Δp is doubled also, but the graph of $\log(\Delta p)$ is only shifted by $\log(2)$ along the pressure axis.

$$\log p_D = \log A + \log \Delta p,$$

$$\log t_D = \log B + \log \Delta t$$

In 1983 Bourdet proposed the use of the logarithmic derivative

$$p' = \frac{\partial \Delta p}{\partial (\ln \Delta t)}$$

Principal ideal is calculate the slope at each pressure point of semi-log plot and plotted on bilogarithmic graph

For exemple, at early time, during the pure wellbore regime, the relationship Equation 1.9 can be expressed as:

$$\log \Delta p = \log \frac{q_B}{24C} + \log \Delta t$$

On log-log scales, the data curve follows a unit slope straight line as described by the early time 45° asymptote on the type curve.

Any flow regime described by either logarithmic or power law

$$P_D = c t_D^n + A$$

$$\frac{\partial P_D}{\partial \ln t_D} = \Delta P_D' = t_D \frac{\partial P_D}{\partial t_D} = t_D c n t_D^{n-1} = c n t_D^n$$

$$\text{WBS with } n=1, \lg \Delta P'_D = \lg \frac{t_D}{c_D}$$

$$\text{LF with } n=0.5 \lg \Delta P'_D = \lg 0.5c_D + 0.5 \lg t_D$$

$$\text{BLF with } n=0.25 \lg \Delta P'_D = \lg 0.25c_D + 0.25 \lg t_D$$

$$\text{SPH with } n=-0.5 \lg \Delta P'_D = \lg(-0.5c_D) + 0.5 \lg t_D$$

$$\text{RF with } P_D = \frac{1}{2} (\ln \frac{t_D}{C_D} + 0.8097 + \ln C_D e^{2s}), \lg \Delta P'_D = \lg \frac{t_D}{2}$$

$$\text{PRF with } n=1 \lg \Delta P'_D = \lg t_D + \dots$$

$$i_{\text{WBS}}=1;$$

$$i_{\text{LF}}=0.5;$$

$$i_{\text{BLF}}=0.25;$$

$$i_{\text{SPH}}=-0.5;$$

$$i_{\text{RF}}=0;$$

$$i_{\text{PSS}}=1;$$

Well with wellbore storage and skin in a homogeneous reservoir

As discussed in former chapter, two characteristic regimes can be observed with this model:

1. *Wellbore storage effect*, with Δp proportional to Δt , and a unit slope log-log straight line on pressure and derivative curves. The wellbore storage coefficient C can be estimated from the corresponding pressure data.

2. *Radial flow* with Δp proportional to $\log(\Delta t)$, and a constant derivative response. Radial flow analysis yields the permeability-thickness product kh and skin factor S .

Example shows at early time a unit slope log-log straight line during the pure wellbore storage effect, and later a stabilization on 0.5 when the radial flow regime is reached. At intermediate time between two characteristic flow regimes, the sand face rate is changing as long as the wellbore storage effect is acting, and the derivative response describes a hump.

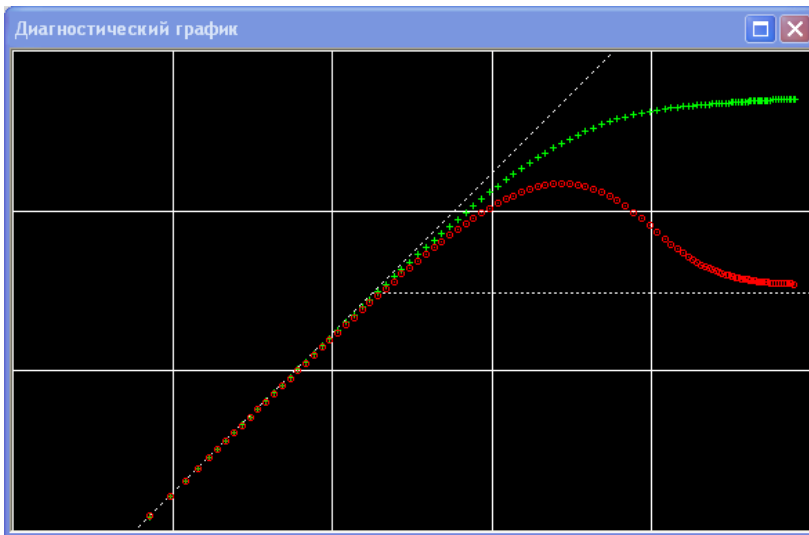


Figure 15. The bottom hole pressure during shut-in period (80 hr) in infinite homogeneous reservoirs (30md).

EFFECT OF RESERVOIR BOUNDARIES

Single sealing fault un homogeneous reservoir

With the sealing fault model, a linear no-flow boundary closes the reservoir in one direction.

The early time part of the well response corresponds to the *infinite reservoir* behavior. During radial flow, the pressure response follows the first semi-log straight line, the derivative follows the first stabilization.

When the influence of the sealing fault is felt, the flow becomes *hemi-radial*, and the apparent mobility is reduced by a factor of two. On semi-log scale, the slope of the straight line doubles and, with the derivative, the curve follows a second stabilization at a level twice the first. In dimensionless terms, the first derivative plateau is at 0.5 and the second at 1.

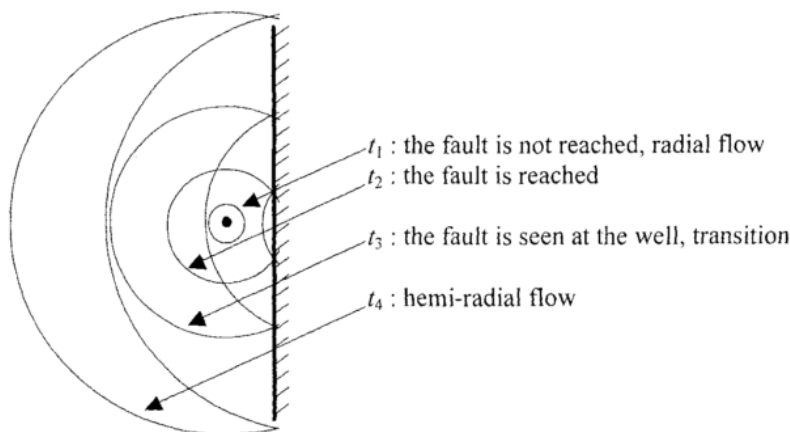


Figure 16. One sealing fault. Drainage radius.

During the hemi-radial flow regime, the pressure changes with the logarithm of the elapsed time but the slope of the semi-log straight line is double ($2m$) that of the infinite acting radial flow (van Everdingen and Hurst, 1949, Homer, 1951)

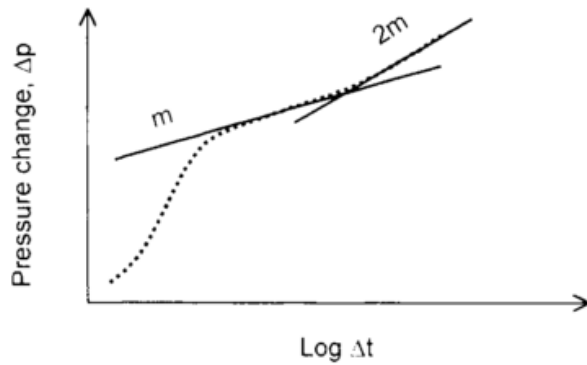


Figure 17. One sealing fault. Specialized analysis on semi-log scale.

On the semi-log plot, two straight lines are present, with a slope respectively m and $2m$. The time intersect Δt . Between the two lines is used to estimate the fault distance L .

$$L = 0.01217 \sqrt{\frac{k\Delta t_x}{\phi\mu c_t}} \quad (14a)$$

$$L = 0.0141 \sqrt{\frac{k\Delta t_x}{\phi\mu c_t}} \quad (14b)$$

Two parallel sealing faults

The well is located between two parallel sealing faults.

This type of configuration frequently corresponds to long narrow reservoirs such as channel sands.

– On the log-log plot, the derivative describes first the wellbore storage effect, then it follows the 0.5 line.

– Later, when the two reservoir boundaries have been reached, the flow lines become parallel to the reservoirs limits, and a linear flow regime is established.

The pressure changes proportionally to, $\sqrt{\Delta t}$, and the derivative follows a *half unit slope* straight line.

– The shape of the transition between radial and linear flow is a function of the well location in the channel. When the well is equidistant from the two boundaries, the transition between radial and linear flow regimes is short.

If the well is closer to one of the two boundaries, the characteristic behavior of *one*

sealing fault is seen before the linear flow. The derivative stabilizes first at 0.5, then 1 and finally it reaches the half unit slope straight line.

Two intersecting sealing fault

The angle of intersection between the two faults can take any value smaller than 180°

The response first describes the infinite reservoir behavior and later, when the two faults are reached, the *fraction* of radial flow limited by the wedge.

In the case of one sealing fault, half of the plane is producing at late times and the semi-log slope doubles, the dimensionless derivative stabilizes at 1. When two intersecting faults limit the drainage area, a smaller fraction of the plane produces: on the semi-log scale, the slope of the straight line is increased by a factor of $360/\theta$ and, with the derivative, the curve follows a *second stabilization* at a level equal to $180/\theta$.

Constant pressure boundary

During drawdown and shut-in periods, the *pressure stabilizes* and the *derivative tends to zero* when the influence of the constant pressure boundaries is felt.

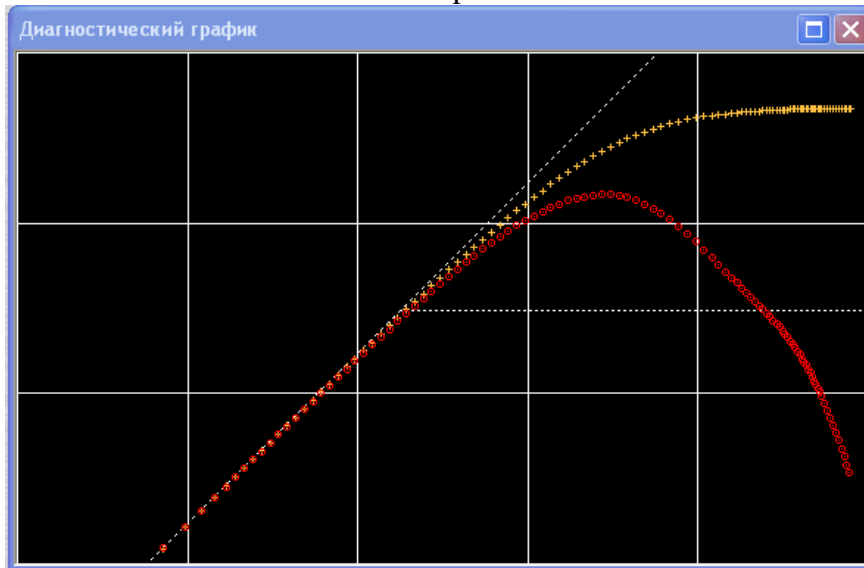


Figure 18. Homogeneous reservoirs ($R=500\text{m}$, $k=30\text{md}$) with constant pressure boundaries .

Closed reservoir

In closed reservoirs, when all boundaries have been reached, the flow regime changes to *pseudo steady state*: i.e at any point in the reservoir the rate of pressure decline is proportional to time. As long as the reservoir is infinite acting, the pressure profile expands around the well during the production (in case of radial flow, the well bottom hole pressure drops with the logarithm of time).

When all boundaries have been reached, the *shape* of the pressure profile becomes *constant* with time, and it simply drops as the reservoir is being depleted. During the pseudo steady state regime, the bottom hole flowing pressure is a linear function of the elapsed time.

During shut-in, the pressure stabilizes in the reservoir and reaches the average reservoir pressure $\bar{p} < p_i$.

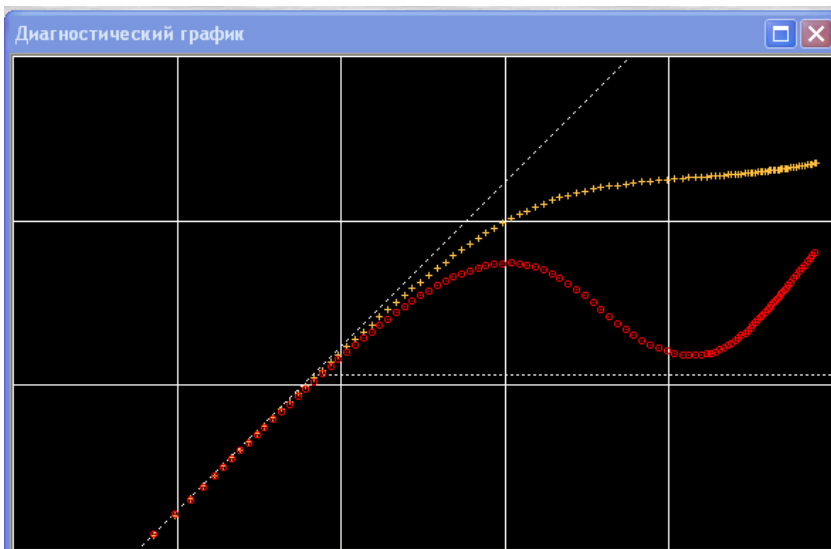


Figure 19. Homogeneous reservoirs ($R=500$ m, $k=30$ md). To maintain reservoir pressure the injection wells is added at a distance of 250 m from the well under investigation.

EFFECT OF RESERVOIR HETEROGENEITIES

Double porosity (porous-fractured reservoir)

The second class of naturally fractured reservoir exhibits two distinct porosity types. The matrix region contains fine pores and often has low permeability. The remaining region – a set of interconnecting fractures, fissures and vugs- has a significant porosity and a high permeability compared with the matrix.

Warren and Root assume that a fractured reservoir can be represented by the system shown on the right side of Fig. The blocks represent the matrix, the space between blocks – fractures. They assume that formation fluid flows from the blocks into the fractures under pseudo steady-state conditions. The fractures carry all fluid to the wellbore. Warren and Root define two characteristics of the fractured system, the ratio of the porosity-compressibility product of the fractures to the total system porosity-compressibility product

$$\omega = \frac{\Phi_2 C_2}{\Phi_1 C_1 + \Phi_2 C_2} = \frac{1}{1 + \Phi_1 C_1 / \Phi_2 C_2} = \frac{1}{1 + \Phi_{ma} C_{ma} / \Phi_f C_f}$$

and the interporosity flow parameter

$$\lambda = \alpha k_{ma} r_c^2 / k_f$$

α - is a matrix to fracture geometric factor with dimension of length^{-2} (m^{-2}).

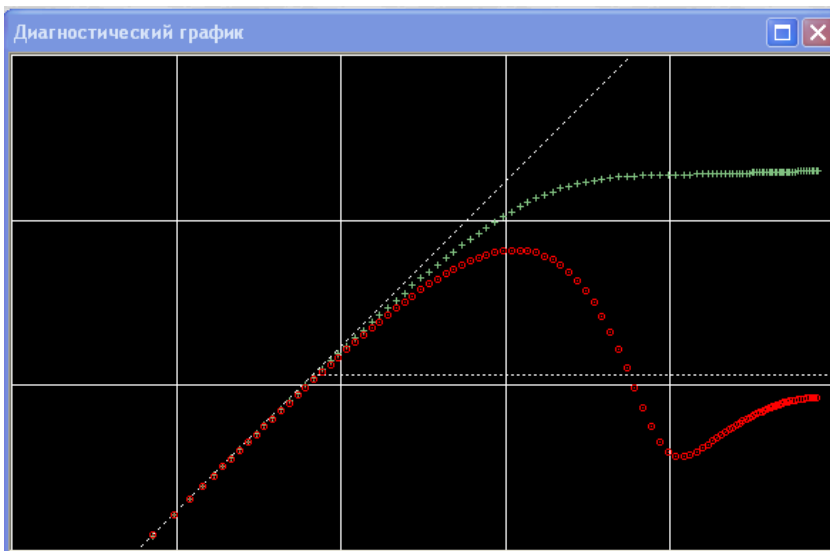


Figure 20. Double porosity reservoir ($k=80$ md, $\omega=0.05$, $\lambda=10^{-7}$).

Composite reservoir

The composite reservoir models consider two distinct media in the reservoir. Each component is defined by a porosity and a permeability, and they are located in different reservoir regions. Radial composite systems: it is assumed that the well is at the center of a circular zone, the outer reservoir structure corresponds to the second element. This geometry is used to describe a radial change of properties, resulting from a change of fluid or formation characteristic. Such change can be man-induced in case of injection wells and in some cases of damaged or stimulated wells. It can also be observed when oil and gas saturations vary around the wellbore, for example when the reservoir produces below bubble point .

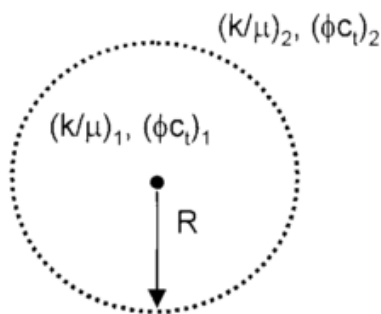


Figure 21. Model for radial composite reservoir.

The changes of reservoir mobility, (k/μ) and storativity (ϕc_i) are expressed with the mobility M and storativity F ratios, defined as region 1 compared to region 2.

$$M = \frac{(k/\mu)_1}{(k/\mu)_2}, \quad F = \frac{(\phi c_i)_1}{(\phi c_i)_2}.$$

A mobility ratio M greater than 1 indicates a decrease of mobility from region 1 to region 2. A decrease of the storage is expressed with the ratio F greater than 1.

With the radial symmetry of the system, the two reservoir regions are seen in sequence:

1. First, the pressure response depends upon the inner zone characteristics, and the well behavior corresponds to a homogeneous reservoir response.
2. When the circular interface is reached, a second homogeneous behavior, corresponding to the outer region, is observed.

Influence of M, derivative responses are presented for different values of the mobility ratio M: the parameters of the well and of the inner zone are constant, the two reservoir regions have the same storativity (F = 1).

For large values of mobility ratio (M=2 and 10, the mobility of the outer region is reduced, and the second derivative plateau is displaced upwards (to 0.5M). The dotted derivative curves show the drawdown response of a well in a closed circle of same radius Ri): it illustrates the limiting case of a zero mobility in the outer zone.

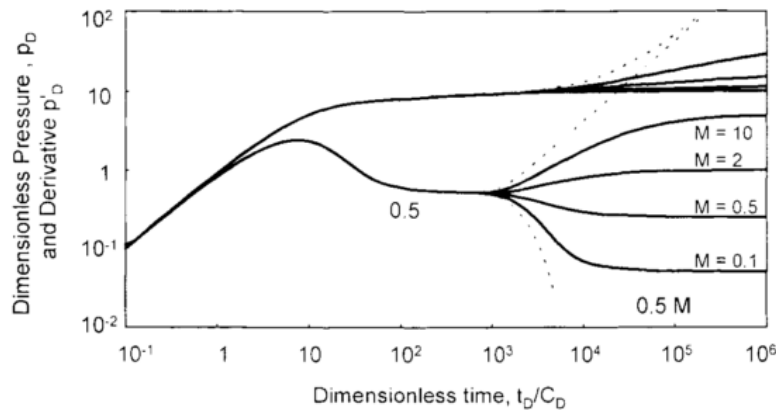


Figure 22. Log-log plot of radial composite responses, changing mobility and constant storativity. P_D versus t_D/C_D. C_D = 100, S = 3, R_o = 700, M = 10, 2, 0.5, 0.1, F = 1. The two dotted curves correspond to the closed and the constant pressure circle solutions.

The mobility ratio M is obtained by comparing the level of the two derivative stabilizations:

$$M = \frac{\Delta p_{1 \text{ stab}}}{\Delta p_{2 \text{ stab}}} \dots$$

The storativity ratio F is in general difficult to access. When the match is

performed on a complete radial composite response generated by computer, F is adjusted from the derivative transition.

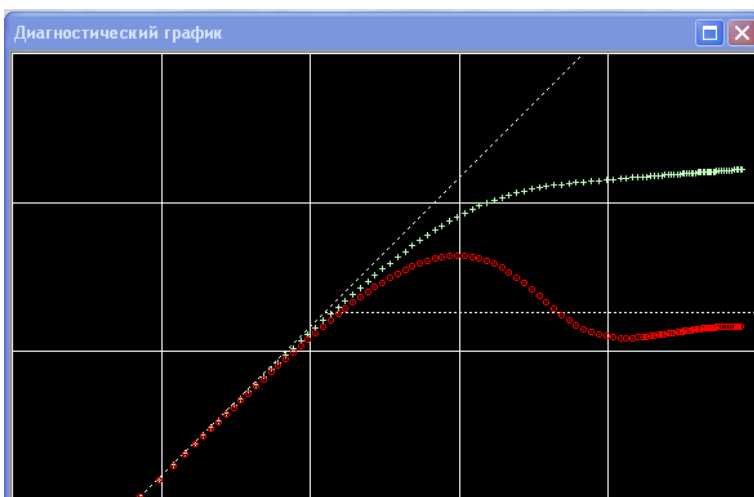


Figure 23. Radial composite reservoir R=300 m, k₁=25 md, k₂=50 мд.

Infinite conductivity or uniform flux vertical fracture

Two characteristic regimes can be observed after the wellbore storage early time effect, as illustrated on Figure 1.12:

1. Linear flow, with Δp proportional to $\Delta t^{1/2}$ and a half unit slope straight line on pressure and derivative log-log curves. The linear flow regime defines the $k(x_f)^2$ product, and therefore the fracture half-length x_f .
2. Pseudo-radial flow regime when the flow lines converge from all reservoir directions. During the pseudo-radial flow regime, the pressure follows a semi-log straight-line behavior, as during the usual radial flow regime towards a cylindrical vertical well. The fracture influence is then described by a geometrical negative skin and the pseudo-radial flow analysis provides the permeability thickness product kh and S_G .

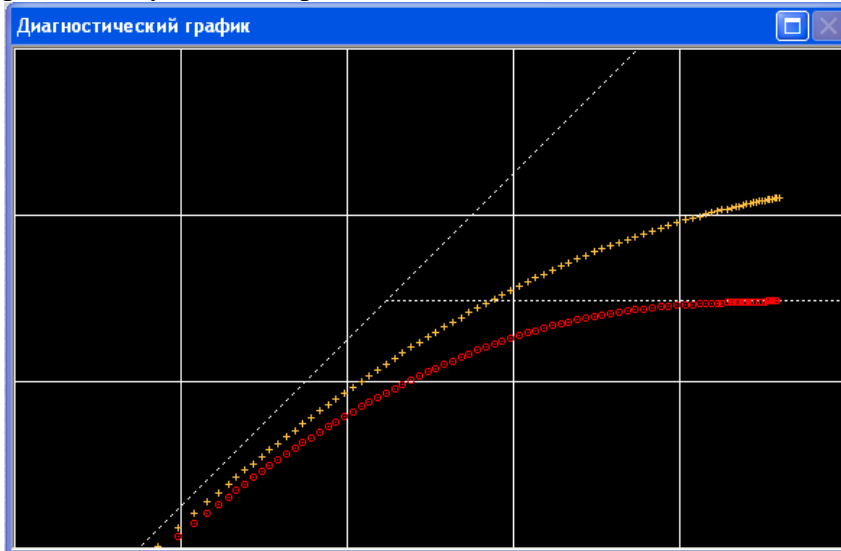


Figure 24. Infinite conductivity vertical fracture $x_{f=}$ 70 м, $k=$ 30 md.

WELLBORE CONDITIONS

Finite conductivity vertical fracture

Three characteristic regimes (Cinco-Ley. and Samaniego-V., 1978) can be observed after the wellbore storage effect:

1. At early times, as long as the fracture tips have not been reached, the combination of fracture linear flow and reservoir linear flow produce the so-called bi-linear flow regime. The pressure change is then proportional to the fourth root of the elapsed time $\sqrt[4]{t}$ and, on the log-log plot, both the pressure and derivative responses follow a quarter unit slope straight line. When present, the bi-linear flow regime gives access to the fracture conductivity $k_f w_f$ (the wellbore pressure is independent of the fracture half-length x_f during bi-linear flow).
2. Later, the pressure behavior becomes equivalent to that of an infinite conductivity fractured well. A linear flow regime can be observed, characterized by the usual pressure and derivative half unit slope log-log straight lines. The fracture half-length x_f can be estimated.
3. Pseudo-radial flow regime, with the derivative stabilization is observed next, to give the permeability thickness product kh and the geometrical skin S_G .

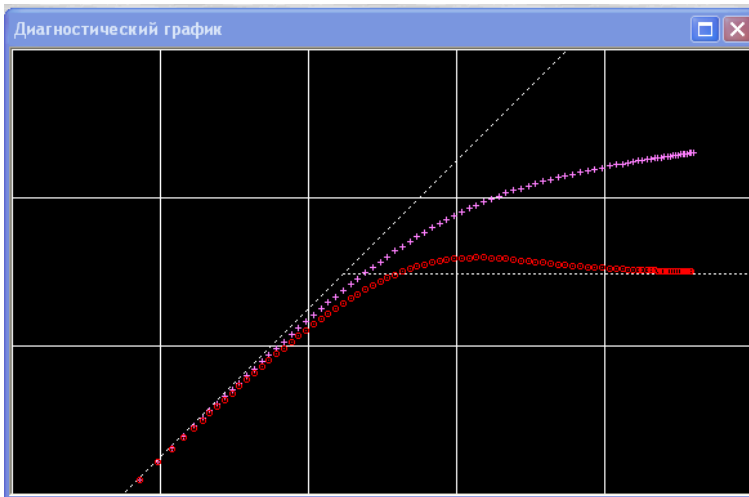


Figure 25. Finite conductivity vertical fracture $k_f w_f = 1524 \text{ md} \cdot \text{m}$

Horizontal well

Advances in drilling and completion technologies have placed horizontal wells among the techniques used to improve production performance. For example in the case of gas cap or bottom water drive, horizontal wells prevent coning without introducing the flow restriction seen in partial penetration wells. Horizontal drilling is also efficient to increase the well surface area for fluid withdrawal, thus improving the productivity.

Model description. We consider the pressure behavior of horizontal wells in homogeneous reservoirs with sealing upper and lower boundaries. The well is strictly horizontal, the penetration half-length is L and z_w defines the distance between the drain hole and the bottom-sealing boundary. The vertical part of the well is not perforated, there is no flow towards the end of the well and the well conductivity is infinite, k_H and k_V are the horizontal and the vertical permeability.

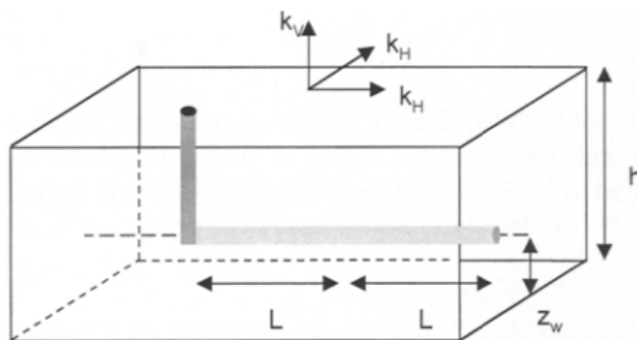


Figure 26. Horizontal well.

In an infinite system, the geometry of the flow lines towards a horizontal well produces a sequence of three typical regimes. On the corresponding pressure and derivative response, three characteristic behaviors are displayed after the wellbore storage unit slope straight line:

1. The first regime is radial flow in the vertical plane. On a log-log derivative plot, the wellbore storage hump is followed by a first stabilization. During this radial flow regime, the

permeability-thickness product $2\sqrt{k_H k_V} L$ is defined with the average permeability in the vertical plane, and the well effective length $2L$.

2. When the sealing upper and lower limits are reached, a linear flow behavior is established. The derivative follows a half-unit slope log-log straight line.

3. Later, the flow lines converge from all reservoir directions towards the well, producing a horizontal radial flow regime. The derivative stabilization corresponds to the infinite acting radial flow in the reservoir, the permeability-thickness product is $k_H h$.

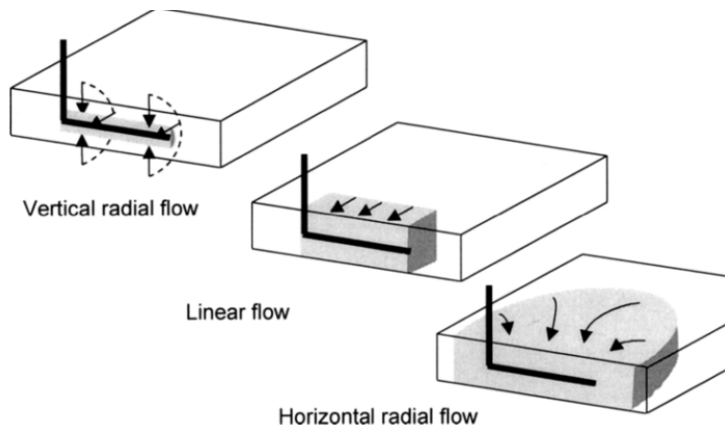


Figure 27. Flow geometry to an horizontal well.

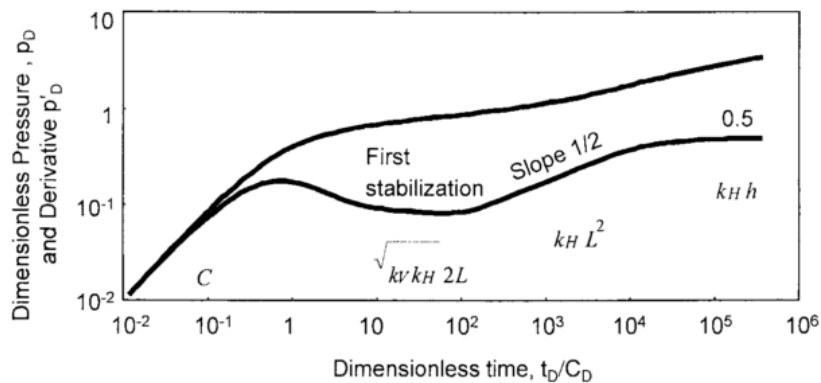


Figure 28. Horizontal well with wellbore storage and skin, homogeneous reservoir. Log-log scales. $C_D = 1000$, $S_w = 0$, $L = 1000\text{ft}$, $h = 100\text{ft}$, $r_w = 0.25\text{ft}$, $Z_w/h = 0.5$, $k_V/k_H = 0.1$.

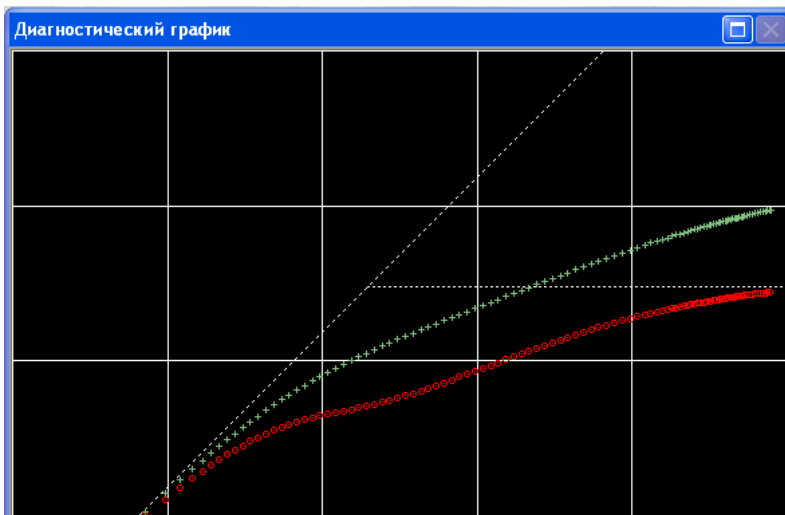


Figure 29. Horizontal well with wellbore storage and skin, homogeneous reservoir. $L = 200$ m, $r_w = 0.1$ m, $Z_w/h = 0.5$, $k_v/k_H = 0.1$.

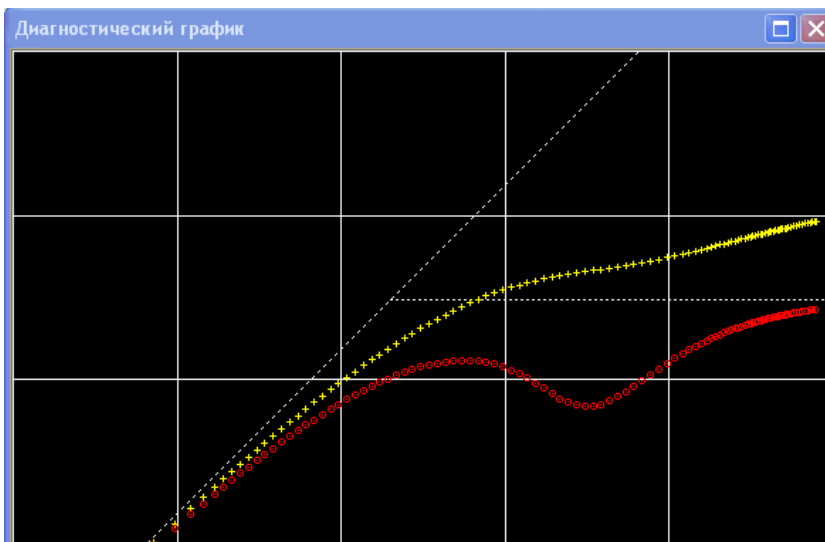


Figure 30. Horizontal well with wellbore storage and skin, double porosity reservoir. $L = 200$ m, $r_w = 0.1$ m, $Z_w/h = 0.5$, $k_v/k_H = 0.1$, $\omega = 0.1$, $\lambda = 10^{-6}$.

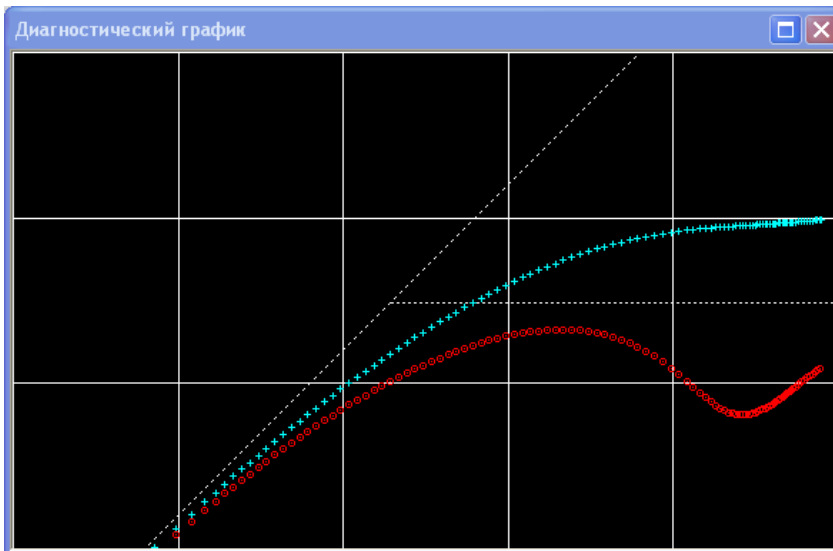


Figure 31. Horizontal well with wellbore storage and skin, double porosity reservoir. $L = 200$ m, $r_w = 0.1$ m, $Z_w/h = 0.5$, $k_v/k_H = 0.1$, $\omega = 0.1$, $\lambda = 10^{-7}$

Changed wellbore storage

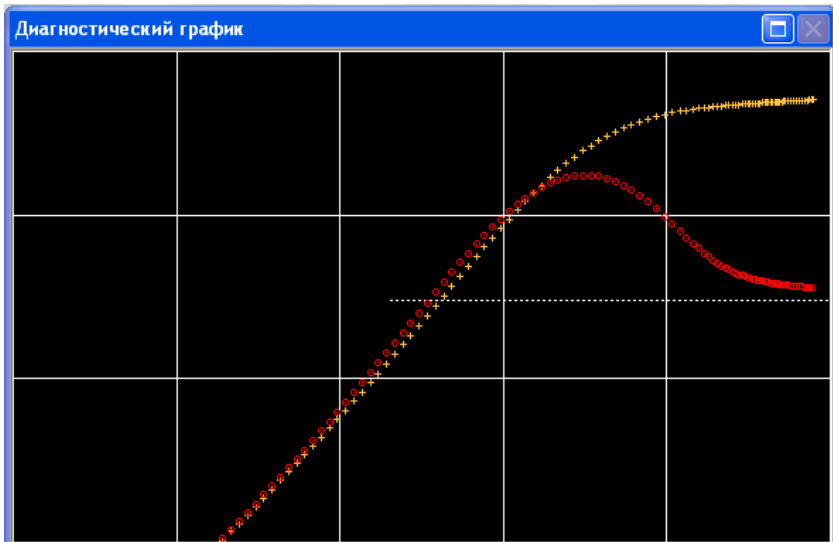


Figure 32. Vertical well with diminishing wellbore storage, homogeneous reservoir $C_i/C_f = 3$, $\Delta t = 2$ hr.

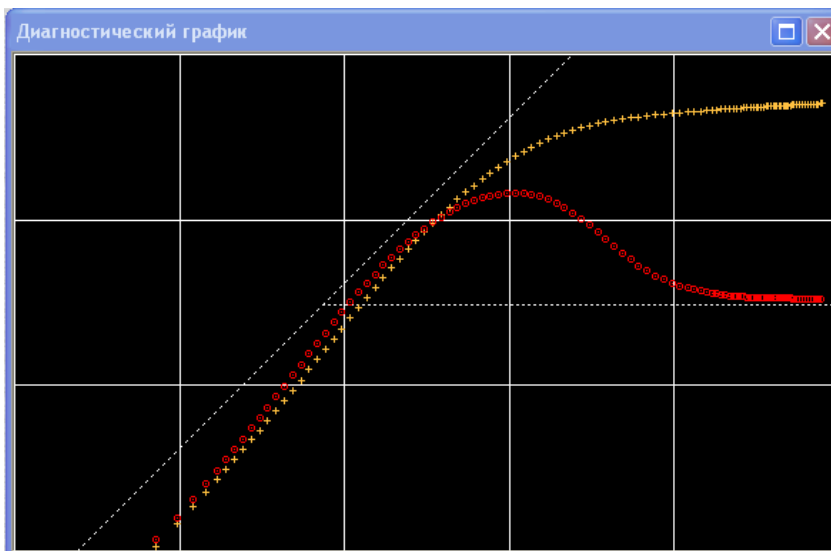


Figure 33. Vertical well with diminishing wellbore storage, homogenous reservoir $C_i/C_f=3$, $\Delta t=0.3$ hr.

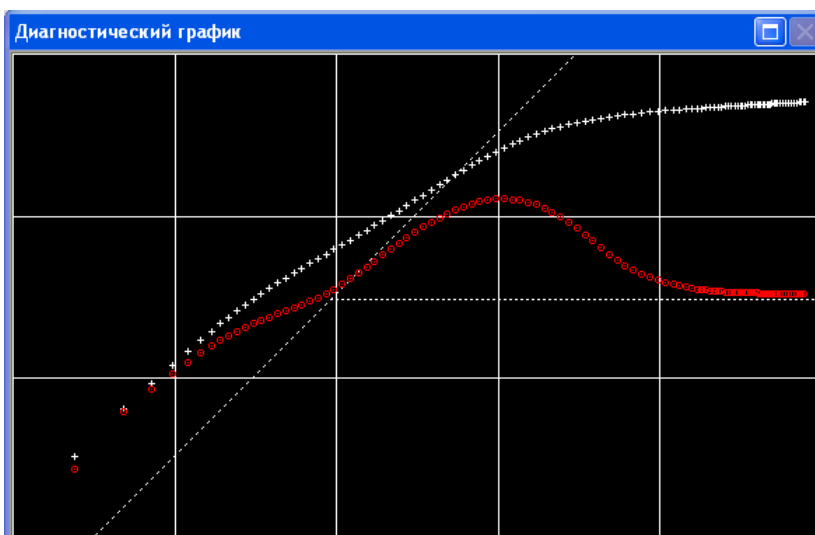


Figure 34. Vertical well with augmenting wellbore storage, homogenous reservoir $C_i/C_f=0.3$, $\Delta t=0.1$ hr.

STEP RATE TEST FOR PRODUCING WELL

Fluid is produced at a series of increasing rates, with each rate preferably lasting the same length of time. In low-permeability formation ($k < 5$ md), each injection rate should last about 1 hour, 30-minute injection times are adequate for $k > 10$ md. As few as four rates may be used, but normally 6-7-8 rates are preferred.

Information obtained from well testing

A step-rate test in an producing well is used to estimate

- well productivity factor (well flow index)

- well productivity factor for gas well
- optimum behavior (pressure, pump regime et c.t.) with low credibility
- reservoir pressure, permeability, skin
- A step-rate injectivity test is normally used to estimate fracture pressure in an injection well. Such information is useful in waterfloods with expensive fluid and is important to avoid injecting through uncontrolled artificially induced fractures.
- A step-rate injectivity test is simple, inexpensive and fast. Fluid is injected at a series of increasing rates, with each rate preferably lasting the same length of time. In low-permeability formation ($k < 5$ md), each injection rate should last about 1 hour, 30-minute injection times are adequate for $k > 10$ md. As few as four rates may be used, but normally 6-7-8 rates are preferred.
- The analysis consists of plotting injection pressure at the end of each rate corresponding injection rate. The plot should have two straight-line segments, as illustrated in fig. 7-30. The break of the line indicates formation fracture pressure. (Unfortunately it can also indicate the breakdown pressure of the cement bond. When the cement bond fails, the slope of the second straight-line segments, usually continues below the fracture pressure as the rate is decreased). The fracture pressure may vary depending on fluid saturation conditions in the formation and long-term variations in reservoir pressure level with time.
- Pressure data taken during each rate may be analyzed with multiple-rate transient technique to estimate formation permeability and skin factor.

NOMENCLATURE

B – formation volume factor, RB/STB

C – wellbore storage coefficient

c_f – formation compressibility, psi^{-1}

c_o – oil compressibility, psi^{-1}

c_t – total compressibility, psi^{-1}

c_w – water compressibility, psi^{-1}

h – formation thickness, ft

h_f – fissures thickness, ft

k – permeability, md

k_f – permeability in fracture, md

k_H – horizontal permeability, md

k_V – vertical permeability, md

m – straight line slope during radial flow, psi/cycle

m_{BLF} – straight line slope during bilinear flow

m_{LFF} – straight line slope during linear flow to a fracture

m_{SPH} – straight line slope during spherical flow

m_{WBS} – straight line slope during wellbore storage effect

p – pressure, psia

\bar{p} – average pressure

q – flow rate, STB/D

r_w – wellbore radius, ft

S – skin coefficient

t – time, hr

Δt – elapsed time or build-up time, hr

x_f —half fracture length, ft
 λ —interporosity flow coefficient
 μ — viscosity, cp
 ϕ – porosity fraction
 ω —storativity ratio in fissured

BIBLIOGRAPHY

1. Bourdet D. Well test analysis: the use of advanced interpretation models/D. Bourdet.- Elsevier, 2002.-426 p
2. Houze O. Dynamic Flow Analysis /Olivier Houze, Didier Viturat, Ole S. Fjaere.- KAPPA, 2007.
3. Эрларгер Р. Гидродинамические исследования скважин /Р. Эрларгер.- М.-Ижевск: Институт компьютерных исследований, 2004. – 467 с. Earlougher, R. C. Advances in well test analysis / Robert C. Earlougher, Jr.- United States : SOCIETY OF PETROLEUM ENGINEERS OF AIME (TX), 1977.-264p.
4. Карнаухов М.Л. Современные методы гидродинамических исследований скважин: справочник инженера по исследованию скважин : уч. пос. для студ. высших учебных заведений/ М. Л. Карнаухов, Е. М. Пьянкова.— Москва: Инфра-Инженерия, 2013 .— 432 с.

SUMMARY

Flow regime

Flow regime	Slope log-log straight line (n)	Specialized analysis with the pressure versus	Dimensionless equations
Radial	0	$\lg t$	$P=A*\lg t+B$
Linear	0.5	$t^{0.5}$	$P=A*t^{0.5}+B$
Bilinear	0.25	$t^{0.25}$	$P=A*t^{0.25}+B$
Spherical	-0.5	$t^{-0.5}$	$P=A*t^{-0.5}+B$
PSS	1	t^1	$P=A*t+B$
Pure wellbore storage effect	1	t^1	$P=A*t+B$

Regime alternation

Well-reservoir- boundary	Regime alternation	On log-log plot (after wellbore storage effect)
Vertical, infinite	Radial	Horizontal straight line n=0
Vertical, one sealing fault	Radial, semi radial	Derivative follows the first stabilization, a second stabilization at a level twice the first
Vertical, infinite conductivity fracture, infinite	Linear, pseudo radial	Half - unit slope straight line, horizontal straight line n=0
Vertical, finite conductivity	Bilinear, linear,	Quarter - unit slope straight line, half -

fracture, infinite	pseudo radial	unit slope straight line, horizontal straight line
Vertical, radial composite reservoir	Radial, radial	Horizontal straight line, switching to other horizontal straight line above or below
Vertical, two parallel sealing fault	Radial, linear	Horizontal straight line, half - unit slope straight line
Horizontal	Radial flow in the vertical plane, linear, pseudo radial	Initial horizontal straight line, half - unit slope straight line, horizontal straight line
Double porosity reservoir		Horizontal straight line, transition valley, horizontal straight line. May be transition valley, horizontal straight line.
Constant pressure boundaries		Derivative tend to zero
Closed reservoir		PSS

APPENDIX

Units

	Oilfield units	Practical metric units
Length	ft	m
Liquid rate	STB/D	m ³ /D
Permeability	md	md
Pressure	psi	bar
Time	hr	hr
Viscosity	cp	cp
Compressibility	psi ⁻¹	bar ⁻¹